Functional Materials

MS.3.P053
Optimization and characterisation of metamorphic buffer layers for extended-InGaAs/InP photodetectors

S. Seifert[1,2], D. Franke[1], D. Zengler[2], F. Kießling[2], M. Lehmann[2]

[1]Fraunhofer Institute for Telecommunications, Heinrich Hertz Institute, Berlin, Germany
[2]TU Berlin, Institut für Optik und Atomare Physik, Berlin, Germany

sten.seifert@hhi.fraunhofer.de
Keywords: photodetector, InGaAs/InP, relaxation, weak-beam dark-field TEM, reciprocal space mapping

For non-contact temperature measurement from 40 °C to 80 °C detectors are needed, which detect thermal radiation up to a wavelength from 2.6 to 2.3 µm. In such detectors the active layer is usually a strongly strained extended-InGaAs (E-InGaAs) grown on InP substrate. The difference of the lattice constant between these both layers is at least $\Delta a/a = +1.5$ % (Fig. 1) which leads to the formation of misfit dislocations. To compensate the strong lattice mismatch between the active layer and substrate a metamorphic buffer layer [1-3] with altering composition is generally used. However, the thickness of total structures in such detectors is usually 15 – 20 µm [4], which is time-consuming and expensive. This work presents the improvement of material quality for E-InGaAs/InP photodetectors, which include metamorphic InAsP buffer layers (Fig. 1). The samples were successively optimized in several parameters such as strain relaxation of metamorphic buffer layers, reduction of total thickness and ideal number of layers.

Metal organic vapor phase epitaxy (MOVPE) growth of E-InGaAs detectors on (001) InP substrate has been performed in a horizontal Aixtron 200 reactor. InAsP metamorphic buffers were grown in order to compensate the lattice mismatch between the E-InGaAs and an InP substrate. Two types of metamorphic buffer layers were grown: step graded and linearly graded buffers. At the step graded buffer layers the number of steps as well as their thickness was varied and optimized by gradually changing the composition resulting in a stepwise adjustment of the lattice constant. In the case of linearly graded buffers the compositions were continuously changed.

To compare step graded with linearly graded buffers, two samples were analyzed by XRD. Figure 2a shows the reciprocal space mapping of sample A and sample B. Sample A has a step graded buffer. Since the layers are quite thick the mosaicity increased and it can be reflected in the broadening of the measured reflection (Fig. 2a) [5]. All measured reflection are on the relaxation line suggesting all the layers are completely relaxed. Sample B has a linearly graded buffer. The measured InGaAs reflection (Fig. 2b) is on the relaxation line. But the last layer before the E-InGaAs layer is not completely relaxed. This is shown in the measured reflection which is marked with 1 (Fig. 2b). Consequently under the used growth conditions, the step graded buffer is more suitable to achieve the required lattice constant.

To investigate the relaxation properties, TEM investigations were carried out on sample A and B. Figures 3a and b show weak-beam dark-field TEM images [6] of samples A and B, respectively. The utilized reflection is a (002). Here, some of the InAsP buffer layers followed by the E-InGaAs active layer are shown. The misfit strain in the buffer layers results in the nucleation of dislocations on a {111} plane. The bright lines in figure 3(a, b) show these misfit dislocations, where some of them bend at the interfaces (Fig. 3a). At the interface region between the last buffer layer to the E-InGaAs active layer no dislocations are observed. In the active layer of sample A the dislocation density is less than $6 \cdot 10^{7}$ cm^{-2}. In sample B at the interface between the last buffer layer and the E-InGaAs layer defects are observed. In the active layer of sample B the dislocation density is more than $7 \cdot 10^{8}$ cm^{-2}. Concluding, the presence of distinct interfaces within the buffer layer is necessary to prevent dislocation lines from advancing throughout the buffer structure towards the device layer.

To derive an ideal relationship between step number and layer thickness a step graded buffer was grown reducing the layer thickness stepwise. These samples were analyzed by XRD. Figure 4 shows the required layer thickness, so that the layer is completely relaxed at a certain strain. It is a minimum layer thickness resulted in a misfit of +0.1%. This is found to be a balance of the critical layer thickness [7, 8] and the reduction of lattice distortion. For the established InAsP buffer a reduced buffer of less than 4 µm overall thickness was grown with a detector structure on top. The total thickness of this structure is 7.5 µm.

1. Ch. Heyn, S. Mendach, S. Loehr, S. Beyer, S. Schnuell, W. Hansen: J. Crystal Growth 251, 832-833 (2003)
2. D.-S. Kim, S.R. Forrest, M.J. Lange, M.J. Cohen, G.H. Olsen, R.J. Menna and R.J. Pfaff: J. Appl. Phys. 80, 6229 (1996)
3. M.K. Hudait, Y. Lin, M.N. Palmisiano and S.A. Ringel: IEEE Electron. Device Lett. 24, 538 (2003)
4. Krier, Y. Mao: Infrared Physics & Technology 38, 397-403 (1997)
5. H. Lin, Y. Huo, Y. Rong, R. Chen, T. I. Kamins, J. S. Harris: J. Crystal Growth 323, 17-20 (2011)
6. E. P. Butler: Micron, Volume 5, Issue 3, 293-305 (1974-1975)
7. J.W. Matthews, A.E. Blakeslee: J. Crystal Growth 27, 118 (1974)
8. R. People, J.C. Bean: Appl. Phys. Lett. 47, 322 (1985); erratum: Appl. Phys. Lett. 49, 229 (1986)

9. This work was conducted within the HINT project (grant # 1N10880) funded by the German Federal Ministry of Education and Research under the KMU-Innovation program

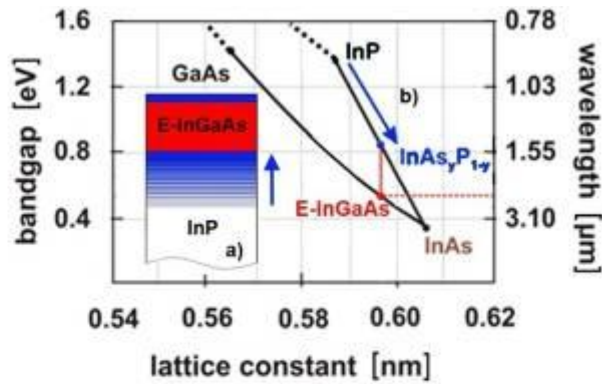

Figure 1. Schematic detector-structure (a). The As-concentration is increased within the buffer layer (b).

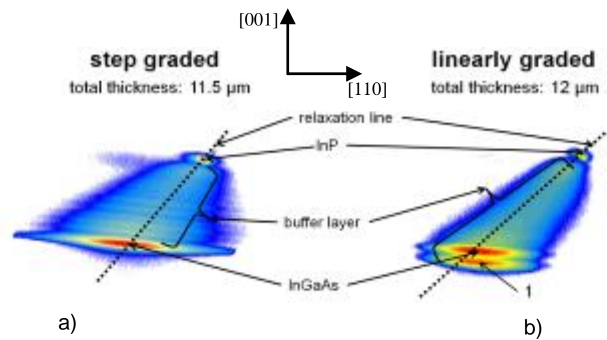

Figure 2. Reciprocal Space Mapping of the (115) reflexes of sample A (a) and sample B (b).

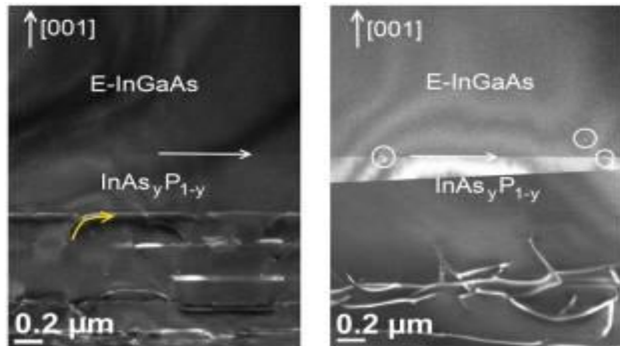

Figure 3. Weak-beam dark-field cross-sectional TEM image of sample A and sample B. The white arrows show the interfaces between the last buffer layer and the E-InGaAs layer (a, b) and the interface between the E-InGaAs layer and the cap layer (b). The bending yellow arrow (a) shows a bending misfit dislocation. The circles (b) show defects in the E-InGaAs layer and at the interface.

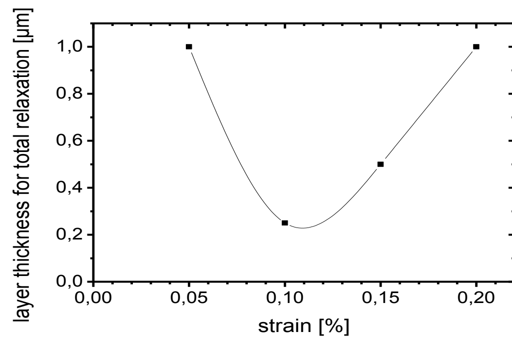

Figure 4. Relationship between strain and required layer thickness so that the layer is completely relaxed.